Int. J. Pharm. Investigation, 2025; 15(3):873-887.
https://www.jpionline.org

Original Article

Design, Synthesis, *in silico* Molecular Docking, ADMET Analysis and *in vitro* Antibacterial Activity of Pyranopyrazole Derivatives as Potent Glucosamine-6-Phosphate Synthase Inhibitor

Prerana Badrinath Jadhav[1,*], Shital Vilas Wagh[2], Manjushri Pratap Dabhade[3]

[1]Department of Pharmaceutical Chemistry, Sanjivani College of Pharmaceutical Education and Research, Sahajanandnagar, Singnapur, Kopargaon, Ahmednagar, Maharashtra, INDIA.
[2]Department of Pharmaceutical Chemistry, Vaishali Tai Jhondhale College of Pharmacy, Dombivali East, Maharashtra, INDIA.
[3]Department of Pharmaceutical Chemistry, R.C. Patel Institute of Pharmaceutical Education and Research, Shirpur, Maharashtra, INDIA.

ABSTRACT

Background: The need for new antibacterial medicines arises from the emergence of antibiotic-resistant bacterial strains. Pyranopyrazole derivatives, known for their diverse biological activities, are investigated for their potential to inhibit glucosamine-6-phosphate synthase, a critical enzyme in bacterial cell wall biosynthesis. **Materials and Methods:** Pyranopyrazole derivatives (SW1-SW10) were synthesized via a one-pot multicomponent reaction. *In silico* ADME and toxicity analyses were conducted to predict pharmacokinetic profiles and potential toxicities. Molecular docking studies were conducted to evaluate binding affinities with glucosamine-6-phosphate synthase (PDB ID: 2VF5). The *in vitro* antibacterial activity was assessed by measuring the zones of inhibition against *Escherichia coli* and *Staphylococcus aureus* at concentrations of 25 µg/mL, 50 µg/mL and 100 µg/mL. **Results:** The docking investigations indicated that SW6 and SW4 exhibited robust binding affinities, with docking scores of -9.4 and -9.0, respectively. *In silico* ADME analysis indicated favorable drug-likeness, with SW1, SW2, SW7 and SW10 meeting all criteria and showing bioavailability scores of 0.55. *In vitro* antibacterial experiments revealed that SW6 displayed the greatest efficacy, with inhibition zones measuring 9.5±0.2 mM, 14.6±0.5 mM and 20.3±0.7 mM against *E. coli* and 10.2±0.3 mM, 15.2±0.6 mM and 21.3±0.8 mM against *S. aureus* at escalating doses. SW4 exhibited comparable efficacy, with inhibition zones measuring 20.8±0.3 mM and 20.2±0.7 mM at 100 µg/mL against *S. aureus* and *E. coli*, respectively. **Conclusion:** The pyranopyrazole derivatives, particularly SW6 and SW4, exhibit strong potential as antibacterial agents. Their high binding affinities and significant *in vitro* antibacterial activity suggest that these compounds could be promising leads for developing new antibacterial therapies targeting antibiotic-resistant strains.

Keywords: Antibacterial Agents, Antibiotic Resistance, Glucosamine-6-Phosphate Synthase, *In silico* ADME, *In vitro* Antibacterial Activity, Molecular Docking, Pyranopyrazole.

Correspondence
Dr. Prerana Badrinath Jadhav
Department Pharmaceutical Chemistry, Sanjivani College of Pharmaceutical Education and Research, Sahajanandnagar, Singnapur, Kopargaon, Ahmednagar-423603, Maharashtra, INDIA.
Email: prerana8487@rediffmail.com

Received: 22-10-2024;
Revised: 18-12-2024;
Accepted: 05-03-2025.

INTRODUCTION

The public's health is seriously threatened by bacterial infections, which can cause a variety of illnesses that can impact different organ systems. These infections are caused by pathogenic bacteria, which invade host tissues and elicit harmful immune responses. *Staphylococcus aureus, Escherichia coli* and *Streptococcus pneumoniae* are common bacterial pathogens that cause a variety of illnesses, from pneumonia and skin infections to sepsis and urinary tract infections. The ability of bacteria to rapidly replicate and adapt to diverse environments, coupled with their propensity to develop resistance to antibiotics, underscores the urgency for novel therapeutic strategies (Besser *et al.*, 2017; Fisher *et al.*, 2017; Principi *et al.*, 2019; Jernigan *et al.*, 2020; Piano *et al.*, 2019). Resistant to Methicillin *Staphylococcus aureus* (MRSA) and multidrug-resistant Gram-negative bacteria have proliferated globally, complicating treatment attempts and driving up morbidity, mortality and healthcare expenditures (Jia *et al.*, 2019; Makabenta *et al.*, 2021). Therefore, the continuous development of novel antibacterial drugs and the investigation of novel molecular targets are essential for the effective management of bacterial infections (Morris *et al.*, 2017).

OPEN ACCESS

Manuscript TECHNOMEDIA

DOI: 10.5530/ijpi.20250157

Glucosamine-6-phosphate Synthase (GlmS) is essential in the bacterial cell wall production process, rendering it a promising target for antibacterial medication development (Khan *et al.*, 2016). This enzyme facilitates the initial step in the production of UDP-N-acetylglucosamine, a crucial precursor for peptidoglycan formation, an essential component of the bacterial cell wall (Bennett *et al.*, 2016; Fikrika *et al.*, 2016). Inhibition of GlmS impedes peptidoglycan production, thereby weakening the bacterial cell wall and leading to cell lysis and mortality (Soukup, 2021). The inhibition of GlmS has shown promise in impairing bacterial growth and survival, particularly in pathogenic strains that rely heavily on robust cell wall synthesis for virulence and resistance to host defenses (Liu *et al.*, 2020). Targeting GlmS offers a dual advantage: it not only hampers bacterial proliferation but also enhances the effectiveness of the host immune response (Beneito-Cambra *et al.*, 2018). This dual mechanism of action highlights the potential of GlmS inhibitors as potent antibacterial agents in the fight against resistant bacterial infections (Silkenath *et al.*, 2023; Foulquier *et al.*, 2020).

Pyranopyrazole derivatives have emerged as a notable category of heterocyclic compounds exhibiting a wide range of biological activity (Yadav *et al.*, 2016). These compounds are structurally diverse and possess unique chemical properties that make them suitable candidates for drug development (Moosavi-Zare *et al.*, 2016). Pyranopyrazoles exhibit significant antibacterial, anti-inflammatory, anticancer and antioxidant properties. The versatility of their biological actions is attributed to their ability to interact with various biological targets. In recent years, the focus has been on exploring their potential as antibacterial agents, given the urgent need for new drugs to combat antibiotic-resistant bacteria (Farooq *et al.*, 2024). Studies have shown that pyranopyrazole derivatives can inhibit key bacterial enzymes, interfere with DNA synthesis and disrupt cell membrane integrity, leading to bacterial cell death (Sharma *et al.*, 2016). The incorporation of pyranopyrazole moieties into drug design not only enhances the antibacterial efficacy but also improves pharmacokinetic properties, making these derivatives promising candidates for further development as novel antibacterial agents (Gadkari *et al.*, 2021).

The main aim of this research is to design, synthesize and assess the biological activity of new pyranopyrazole derivatives as possible inhibitors of glucosamine-6-phosphate synthase. This study intends to utilize *in silico* molecular docking and ADMET analysis to forecast the interactions and pharmacokinetic profiles of the synthesized drugs. The research aims to evaluate the *in vitro* antibacterial efficacy of these compounds against multiple harmful bacterial strains. By targeting glucosamine-6-phosphate synthase, this research endeavors to identify potent antibacterial agents that can contribute to the development of new therapies for combating bacterial infections, particularly those caused by antibiotic-resistant strains.

MATERIALS AND METHODS

Materials

The chemicals and solvents utilized in this investigation obtained from Sciquaint Innovation Pvt. Ltd., in India. A variety of spectroscopic methods was utilized to thoroughly characterize the produced compounds. FTIR spectra were obtained utilizing an alpha Bruker eco ATR instrument, whereas 1H NMR spectra were collected with a Bruker AM-300 spectrophotometer, using Tetramethylsilane (TMS) as the internal reference. Deuterated solvents, such as DMSO and chloroform, were employed for spectroscopic measurements, with chemical shifts reported as delta values relative to TMS. The melting points were ascertained utilizing a digital Gallen Kemp melting point device. The final synthesized compounds were recrystallized using suitable solvents to guarantee superior purity. The processes were observed via Thin-Layer Chromatography (TLC), with silica gel-60 HF254 plates as the stationary phase for compound separation and a solvent mixture of methanol and chloroform in a 1:9 ratio.

Methods

Ligand Preparation

The proposed ligands of pyranopyrazole derivatives were prepared using Chem3D (v.16.0) and ChemDraw (v.16.0) software. Chem Office's MM2 force field approach was utilized to optimize the initial shape of these ligands. This stage guarantees that the ligands achieve a stable conformation appropriate for research on docking (Butt *et al.*, 2020). Following optimization, the ligands were given Gasteiger charges to appropriately represent their electronic distribution, a crucial component of effective docking. This ligand preparation technique has been successfully applied in research of a similar kind and is essential to ensuring the validity of the docking data (Forli *et al.*, 2016; Ravi *et al.*, 2016).

Selection Target receptor

In this study, Glucosamine-6-phosphate Synthase (GlmS), with the PDB ID: 2VF5 (Figure 1), was selected as the target receptor for evaluating the antibacterial potential of our synthesized pyranopyrazole derivatives. GlmS is a crucial enzyme in the bacterial cell wall biosynthesis pathway, catalyzing the first step in the synthesis of UDP-N-acetylglucosamine, a key precursor for peptidoglycan formation (Niu *et al.*, 2018). Inhibiting GlmS disrupts this pathway, leading to impaired cell wall synthesis and, consequently, bacterial cell death (Li *et al.*, 2020). The Mechanism of Action (MOA) positions GlmS as a compelling target for the creation of novel antibacterial drugs, especially given the increasing prevalence of antibiotic resistance. The choice of GlmS for our research is predicated on its critical function in bacterial viability and its promise as a novel target for antibacterial pharmacotherapy. By focusing on this enzyme, we aim to identify pyranopyrazole derivatives that can effectively inhibit GlmS,

offering a new approach to combating bacterial infections (Li *et al.*, 2020).

Protein Preparation

The crystal structure of Glucosamine-6-Phosphate synthase (PDB ID: 2VF5) was obtained from the Protein Data Bank (www.rcsb.org) (Gaillard T, 2018). To guarantee that the protein was ready for docking, a number of procedures were engaged in its preparation (Eberhardt *et al.*, 2021). At first, every water molecule in the crystal structure was eliminated. Subsequently, absent hydrogen atoms were appended, an essential measure for precisely depicting the protein's three-dimensional configuration (El-Hachem *et al.*, 2017). The proteins were produced using the Discovery Studio Visualizer (v.4.5). The potential binding pocket where the ligands and the target bind were determined by the integrated active site detection method in the Discovery Studio Visualizer (v.4.5) program (Agrwal *et al.*, 2022; Abdelatty *et al.*, 2023).

Molecular Docking

Molecular docking was performed with AutoDock Vina, version 1.2.0. This procedure was conducted to assess the interactions and binding affinities between the optimized ligands and glucose-6-phosphate synthase. A grid box measuring 20x20x20 Å was used to define the active site of the protein. It was centered on the coordinates x=-11.343897, y=6.133868 and z=-23.338819. The catalytic site residues were covered by this grid, guaranteeing that the docking simulations concentrate on the desired area (Abdelatty *et al.*, 2023). The docking procedure was carried out and the docking scores-which represent the ligands' binding affinity to the protein-were used to evaluate the outcomes (Fouda *et al.*, 2022). For further examination, the poses with the best docking were selected. The visualization and analysis of the protein-ligand complexes were conducted with Discovery Studio Visualizer (v.4.5), while LigPlot+ (v.2.2) was employed to generate 2D interactions that highlighted the essential interactions between the ligands and protein residues. This methodology follows the established protocols in molecular docking studies, producing results that are reliable and informative (Eberhardt *et al.*, 2021).

Drug likeness and *in silico* ADMET prediction

The ADMET profiles of 10 Pyranopyrazole derivatives were evaluated using SwissADME, a comprehensive online tool for ADME prediction (http://www.swissadme.ch) (Damayanti *et al.*, 2022). The drug-likeness of these compounds was assessed based on Lipinski's Rule of 5 (Batool *et al.*, 2024). This regulation delineates essential criteria for New Molecular Entities (NMEs), positing that molecules surpassing thresholds of five hydrogen bond donors, ten hydrogen bond acceptors, a molecular weight exceeding 500 Da and a Calculated Log P (CLog P) greater than five are likely to demonstrate inadequate absorption or permeation (Kurma *et al.*, 2024; Allayeh *et al.*, 2024). As a result, compounds that do not meet these requirements are usually considered inappropriate for oral bioavailability as pharmaceuticals (Abdelazeem *et al.*, 2024).

Toxicity Analysis

ProTox-II, a web-based tool designed for predicting toxicity (https://tox-new.charite.de/protox_II/), was utilized to conduct the toxicity analysis of the compounds. This analysis included a thorough assessment of a number of important toxicity parameters (Banerjee *et al.*, 2022). Each compound's toxicity class was ascertained by calculating its Lethal Dose 50 (LD_{50}) values, which are expressed in mg/kg and provide a quantitative indicator of acute toxicity (Banerjee *et al.*, 2018). Furthermore, a percentage evaluation of these values' prediction accuracy was conducted. The evaluation of hepatotoxicity, carcinogenicity, immunotoxicity, mutagenicity and cytotoxicity were among the additional toxicity assessments (Oner *et al.*, 2023). Every parameter was carefully examined and a key component of this evaluation was the likelihood of occurrence. In this situation, ProTox-II made it possible to obtain a thorough and accurate toxicity profile for every substance, which greatly aided in understanding the compound's safety profile for possible therapeutic uses.

Synthesis

Synthesis of Pyranopyrazole derivatives (SW1-SW10)

A reaction mixture was made up of ethyl benzoylacetate (1 mmol), substituted phenyl hydrazine (Ar, 1 mmol) shown in Table 1 and Figure 2, formaldehyde (1 mmol), malononitrile (1 mmol) and a catalyst made up of acetic acid, thiourea and $NH_4CH_3CO_2$ in a 6:4:1 ratio (0.5 g) (Abdelatty *et al.*, 2023). The mixture was agitated at ambient temperature for roughly 15 min. After the reaction was completed, as verified by TLC, the solid residue underwent filtration, was washed with water and was subsequently dried to obtain the pure product. The initial product (1 mmol) was refluxed again for an additional 2 hr with the substituted benzaldehyde (Ar1, 1 mmol) as detailed in Table 1 (Mamaghani *et al.*, 2021). Once the reaction was cool, ice was added to precipitate it. 1H NMR, FTIR and MS were used to confirm the compounds (Gadkari *et al.*, 2021).

Detailed mechanism of action was given in Figure 3.

Same procedure was followed for all derivatives

SW1: Yield: 87.54%, MP: 179-181°C, R_f value: 0.76, FTIR (cm^{-1}): 3307.54 (NH stretching), 3063.12 (Aromatic C-H stretching), 2962.85 (Aliphatic C-H stretching), 2233.47 (C≡N stretching), 1604.29 (C=C aromatic stretching), 1508.67 (C=N stretching), ^{1}H NMR (δ ppm): 7.25-7.85 (Aromatic H), 3.82 (OCH_3), 2.33 (CH_3), m/s: 494.98.

SW2: Yield: 89.59%, MP: 173-175°C, R_f value: 0.78, FTIR (cm^{-1}): 3310.28 (NH stretching), 3068.49 (Aromatic C-H stretching),

2860.13 (Aliphatic C-H stretching), 2240.59 (C≡N stretching), 1602.87 (C=C aromatic stretching), 1502.98 (C=N stretching), ^{1}H NMR (δ ppm): 7.15-7.95 (Aromatic H), 3.89 (OCH_3), 2.27 (CH_3), m/s: 494.98.

SW3: Yield: 64.34%, MP: 173-188°C, R_f value: 0.88, FTIR (cm^{-1}): 3323.27 (N-H stretching), 3034.48 (Aromatic C-H stretching), 2926.37 (Aliphatic C-H stretching), 2854.61 (Aliphatic C-H stretching), 2228.70 (C≡N stretching), 1739.05 (Possible C=O stretching), 1605.98 (C=C stretching), 1525.93 (N-O asymmetric stretch), 1347.69 (N-O symmetric stretch), 1255.48 (C-N stretching), 1028.22 (C-N stretching), 831.05 (Aromatic C-H bending), 756.63 (Aromatic C-H bending), 698.80 (Out-of-plane bending of aromatic C-H), ^{1}H NMR (δ ppm): 2.50 (Singlet), 3.36 (Singlet), 6.59-7.98 (Multiplet), m/s: 530.37.

SW4: Yield: 73.63%, MP: 190-194°C, R_f value: 0.93, FTIR (cm^{-1}): 3428.23 (O-H stretching), 2926.45 (Aliphatic C-H stretching), 2854.43 (Aliphatic C-H stretching), 2231.55 (C≡N stretching), 1628.92 (C=C stretching), 1583.46 (N=O asymmetric stretch), 1511.73 (N=O asymmetric stretch), 1341.44 (N=O symmetric stretch), 1248.54 (C-O stretching), 1028.34 (C-O stretching), 835.82 (Aromatic C-H out-of-plane bending), 818.02 (Aromatic C-H out-of-plane bending), 745.52 (Aromatic C-H out-of-plane bending), ^{1}H NMR (δ ppm): 2.50 (Singlet), 3.37 (Singlet), 6.00-7.00 (Multiplet), 7.00-8.00 (Multiplet), m/s: 552.50.

SW5: Yield: 67.28%, MP: 194-198°C, R_f value: 0.89, FTIR (cm^{-1}): 3318.45 (NH stretching), 3072.30 (Aromatic C-H stretching), 2855.67 (Aliphatic C-H stretching), 2218.04 (C≡N stretching), 1598.33 (C=C aromatic stretching), 1511.23 (C=N stretching), ^{1}H NMR (δ ppm): 7.05-8.05 (Aromatic H), 3.76 (OCH_3), 2.40 (CH_3), m/s: 505.53.

SW6: Yield: 82.75%, MP: 177-181°C, R_f value: 0.77, FTIR (cm^{-1}): 3329.34 (O-H stretching), 3061.02 (Aromatic C-H stretching), 2843.32 (Aliphatic C-H stretching), 2228.44 (C≡N stretching), 1669.50 (C=O stretching), 1618.44 (C=C stretching), 1595.24 (N=O asymmetric stretch), 1506.42 (N=O asymmetric stretch), 1344.26 (N=O symmetric stretch), 1253.84 (C-O stretching), 1170.14 (C-O stretching), 1026.34 (C-N stretching), 831.77 (Aromatic C-H out-of-plane bending), 756.73 (Aromatic C-H out-of-plane bending), 693.74 (Aromatic C-H out-of-plane bending), ^{1}H NMR (δ ppm): 2.30 (Singlet), 3.35 (Singlet), 6.00-7.20 (Multiplet), 7.20-8.00 (Multiplet), m/s: 552.50.

SW7: Yield: 89.71%, MP: 178-180°C, R_f value: 0.74, FTIR (cm^{-1}): 3299.76 (NH stretching), 3060.88 (Aromatic C-H stretching), 2852.16 (Aliphatic C-H stretching), 2226.30 (C≡N stretching), 1610.42 (C=C aromatic stretching), 1506.38 (C=N stretching), ^{1}H NMR (δ ppm): 7.20-7.90 (Aromatic H), 3.68 (OCH_3), 2.38 (CH_3), m/s: 533.59.

SW8: Yield: 92.83%, MP: 186-190°C, R_f value: 0.79, FTIR (cm^{-1}): 3304.32 (NH stretching), 3065.75 (Aromatic C-H stretching), 2958.25 (Aliphatic C-H stretching), 2221.55 (C≡N stretching), 1606.78 (C=C aromatic stretching), 1504.92 (C=N stretching), ^{1}H NMR (δ ppm): 7.28-8.00 (Aromatic H), 3.85 (OCH_3), 2.45 (CH_3), m/s: 507.03.

SW9: Yield: 64.44%, MP: 193-196°C, R_f value: 0.79, FTIR (cm^{-1}): 3322.13 (NH stretching), 3070.02 (Aromatic C-H stretching), 2954.17 (Aliphatic C-H stretching), 2228.75 (C≡N stretching), 1612.66 (C=C aromatic stretching), 1509.51 (C=N stretching), ^{1}H NMR (δ ppm): 7.22-7.92 (Aromatic H), 3.90 (OCH_3), 2.29 (CH_3), m/s: 478.98.

SW10: Yield: 79.38%, MP: 201-205°C, R_f value: 0.88, FTIR (cm^{-1}): 3315.89 (NH stretching), 3062.11 (Aromatic C-H stretching), 2857.43 (Aliphatic C-H stretching), 2235.10 (C≡N stretching), 1608.34 (C=C aromatic stretching), 1507.88 (C=N stretching), ^{1}H NMR (δ ppm): 7.10-7.98 (Aromatic H), 3.74 (OCH_3), 2.36 (CH_3), m/s: 430.51.

In vitro Antibacterial activity

The antibacterial effectiveness of the test compounds was assessed *in vitro* utilizing the agar well diffusion method against the bacterial strains *Escherichia coli* and *Staphylococcus aureus*. Single isolated colonies of these organisms were inoculated into Luria-Bertani broth, followed by incubation at 37°C for 18-24 hr to achieve log-phase growth. The bacterial inoculum was standardized to 0.5 McFarland turbidity, corresponding to approximately 1.5×10^8 colony-forming units per millilitre. The bacterial suspension was uniformly applied to Mueller-Hinton agar plates, creating wells approximately 6 mM in diameter. Solutions were evaluated at concentrations of 25, 50 and 100 µg/mL in the wells, with conventional antibiotics serving as positive controls and the solvent alone as negative controls. Following the incubation of the agar plates at 37°C for 18-24 hr, the zones of inhibition surrounding each well were meticulously examined and quantified. The enlarged zones of inhibition indicate improved antibacterial effectiveness of the evaluated drugs. The zones of inhibition generated by the test compounds were analysed in comparison to the control groups to evaluate their relative efficacy

Table 1: Derivatives of Pyranopyrazole.

Sl. No.	Label	Ar	Ar^1
1	SW1	2	2
2	SW2	2	2
3	SW3	2	2
4	SW4	2	2
5	SW5	2	2
6	SW6	2	2
7	SW7	2	2
8	SW8	2	2
9	SW9	2	2
10	SW10	2	2

against the bacterial strains. Additional statistical analysis was performed to ascertain the minimum inhibitory concentrations and other pertinent parameters related to antibacterial activity.

RESULTS

Chemistry of Pyranopyrazole

Pyranopyrazole derivatives represent a significant class of heterocyclic compounds characterized by a fused pyran and pyrazole ring system. The structure Pyranopyrazole derivatives of the current research (Figure 1) includes a pyran ring fused with a pyrazole ring and these derivatives often exhibit a Cyano group (-CN) and an Aryl group (Ar) at specific positions, contributing to their diverse biological activities. The synthesis of these compounds occurs via a one-pot, multicomponent reaction that incorporates ethyl benzoylacetate, substituted phenyl hydrazines, formaldehyde and malononitrile, utilizing a catalytic system comprising acetic acid, thiourea and ammonium acetate. This effective domino cyclization mechanism concurrently generates both the pyran and pyrazole rings. Pyranopyrazole derivatives exhibit a wide range of biological actions, including antibacterial, anti-inflammatory, anticancer and antioxidant effects. Their varied chemical structure enables multiple substitutions, increasing their potential as candidates for drug development.

The Structure-Activity Relationship (SAR) of pyranopyrazole derivatives (Figure 4) highlights the impact of different substituents on their biological activity. Modifications on the aryl group at position 1 (Ar) influence binding affinity and specificity, with electron-withdrawing groups enhancing activity. The cyano group at position 2 is crucial for forming hydrogen bonds with target proteins, increasing inhibitory potency. Substituents on the aryl group at position 3 (Ar_1) affect solubility and metabolic stability, optimizing pharmacokinetic profiles. The nitrogen atom in the pyrazole ring is essential for maintaining structural integrity and proper orientation for binding. Modifications to the pyran ring can alter molecular conformation and flexibility, affecting the compound's fit in the enzyme's binding pocket and influencing biological activity. By systematically varying these substituents, researchers can design more potent and selective pyranopyrazole-based inhibitors.

DISCUSSION

The Lipinski rule of five and Veber's rule were considered for assessing the druglikeness of pyranopyrazole derivatives synthesized in Table 2. According to Lipinski's rule of five, the compound will be drug-like if it has a molecular weight (Mol. Wt.) below 500 g/mol, with a logP value (M Log P) below 5, no more than 5 Hydrogen Bond Donors (HBD), maximum 10 Hydrogen Bond Acceptors (HBA) and no more than one violation of these parameters. The overall recommendations are that the majority of compounds are in good agreement with Lipinski's rule set. More precisely, SW1, SW2, SW5, SW7, SW9 and SW10 feature one violation-essentially because their logP values slightly exceed the threshold of 5. On the contrary, SW3, SW4, SW6 and SW8

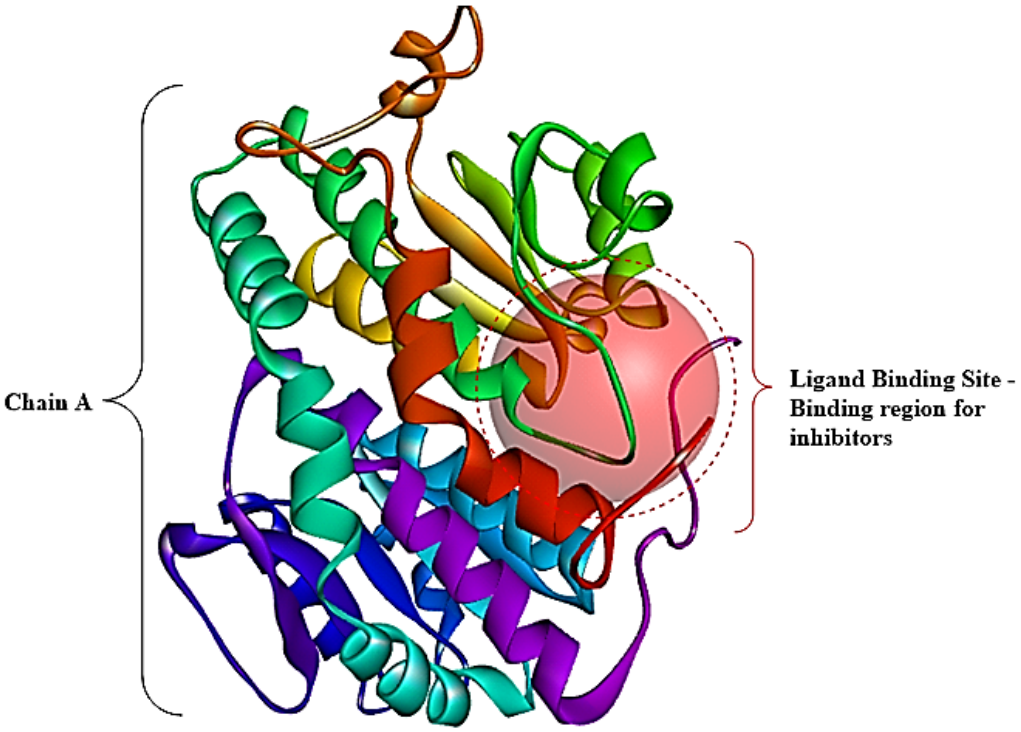

Figure 1: Crystal structure of Glucosamine-6-phosphate synthase (GlmS) (PDB ID: 2VF5).

Calculations of Lipinski's rule of Five and Druglikeness

Table 2: Lipinski rule and Druglikeness analysis of designed.

Compound Codes	Lipinski rule of five					Veber's rule	
	M Log P	Mol. Wt. (g/mol)	HBA	HBD	Violations	TPSA (Å^2)	No. of rotatable bonds
SW1	4.64	494.97	5	0	1	72.43	5
SW2	4.64	494.97	5	0	1	72.43	5
SW3	4.35	530.36	6	0	2	109.02	5
SW4	1.82	552.49	10	0	2	173.30	8
SW5	3.30	505.52	7	0	1	118.25	6
SW6	1.82	552.49	10	0	2	173.30	8
SW7	3.68	533.58	7	0	1	118.25	8
SW8	5.56	507.03	4	0	2	63.20	6
SW9	5.18	478.97	4	0	1	63.20	5
SW10	4.53	430.50	4	0	1	63.20	5

Mol. Wt.-Molecular weight, HBA-Hydrogen bond acceptors, HBD-Hydrogen bond donor, TPSA-Topological Polar Surface Area.

In silico ADME properties

Table 3: *In silico* ADME properties of designed pyranopyrazole derivatives.

Compound codes	Pharmacokinetics									Drug-likeness			
	GI abs.	BBB pen.	P-gp sub.	CYP1A2	CYP2C19	CYP2C9	CYP2D6	CYP3A4	Log K_p (skin permeation, cm/s)	Ghose	Egan	Muegge	Bioavailability Score
				Inhibitors									
SW1	High	No	No	No	Yes	Yes	No	No	-4.66	3	1	1	0.55
SW2	High	No	No	No	Yes	Yes	No	No	-4.66	3	1	1	0.55
SW3	Low	No	No	No	Yes	Yes	No	No	-4.79	3	1	1	0.17
SW4	Low	No	No	No	No	yes	No	Yes	-6.23	2	1	1	0.17
SW5	Low	No	No	No	Yes	Yes	No	No	-5.29	3	0	1	0.55
SW6	Low	No	No	No	No	yes	No	Yes	-6.23	2	1	1	0.17
SW7	Low	No	No	No	Yes	Yes	No	No	-4.85	3	1	1	0.55
SW8	Low	No	Yes	Yes	No	No	No	No	-3.84	3	1	1	0.17
SW9	Low	No	No	No	Yes	Yes	No	No	-4.24	2	1	1	0.55
SW10	High	No	No	No	Yes	Yes	No	No	-4.64	1	1	1	0.55

GI: Gastrointestinal; **BBB:** Blood-brain barrier.

have two violations; essentially because of either higher molecular weights or more than allowed hydrogen bond acceptors that may indicate potential bioavailability problems or solubility issues. Veber's rule, measuring oral bioavailability, says compounds must have a TPSA<140 Å^2 and <10 rotatable bonds. SW3, SW4 and SW6 have > the TPSA limit of 109.02 Å^2, 173.30 Å^2 and 173.30 Å^2, respectively that most likely impact their permeability Table 2. At last, compounds SW4, SW6 and SW7 contain an increased number of rotatable bonds (8), which might influence their flexibility and consequently their oral bioavailability. Compounds SW1, SW2, SW5, SW8, SW9 and SW10 follow Veber's rules, which is indicative of a better chance of oral bioavailability. Taking into consideration all the above, whereas many derivatives seem to be drug-like, the effort to minimize violations in lipophilicity and hydrogen bond acceptors might help enhance the drug-likeness and effectiveness as antibacterial agents. The crystal structure of GlmS (Figure 1) and the fact that a critical enzyme in bacterial cell wall biosynthesis is targeted further support the rational design of such derivatives.

In silico Toxicity analysis

Table 4: Predicted toxicity of molecules.

Compound codes	Parameters							
	LD_{50} (mg/kg)	Toxicity class	Prediction accuracy (%)	Hepatotoxicity	Carcinogenicity	Immunotoxicity	Mutagenicity	Cytotoxicity
				(Probability)				
SW1	1000	4	54.26	A (0.56)	I (0.60)	I (0.65)	I (0.52)	I (0.67)
SW2	1000	4	54.26	A (0.56)	I (0.60)	I (0.53)	I (0.52)	I (0.67)
SW3	1000	4	54.26	A (0.55)	A (0.53)	A (0.83)	A (0.80)	I (0.72)
SW4	900	4	23.78	A (0.56)	A (0.55)	A (0.94)	A (0.79)	I (0.69)
SW5	1190	4	100	A (0.69)	I (0.62)	A (0.96)	I (0.97)	I (0.93)
SW6	900	4	23.32	A (0.56)	A (0.55)	A (0.94)	A (0.79)	I (0.69)
SW7	900	4	54.26	A (0.53)	A (0.55)	A (0.96)	A (0.71)	I (0.67)
SW8	1000	4	54.26	I (0.50)	I (0.61)	I (0.84)	I (0.57)	I (0.70)
SW9	1000	4	54.26	A (0.51)	I (0.59)	I (0.87)	I (0.58)	I (0.70)
SW10	900	4	54.26	A (0.50)	A (0.61)	I (0.97)	I (0.56)	I (0.69)

A=Active, I=Inactive.

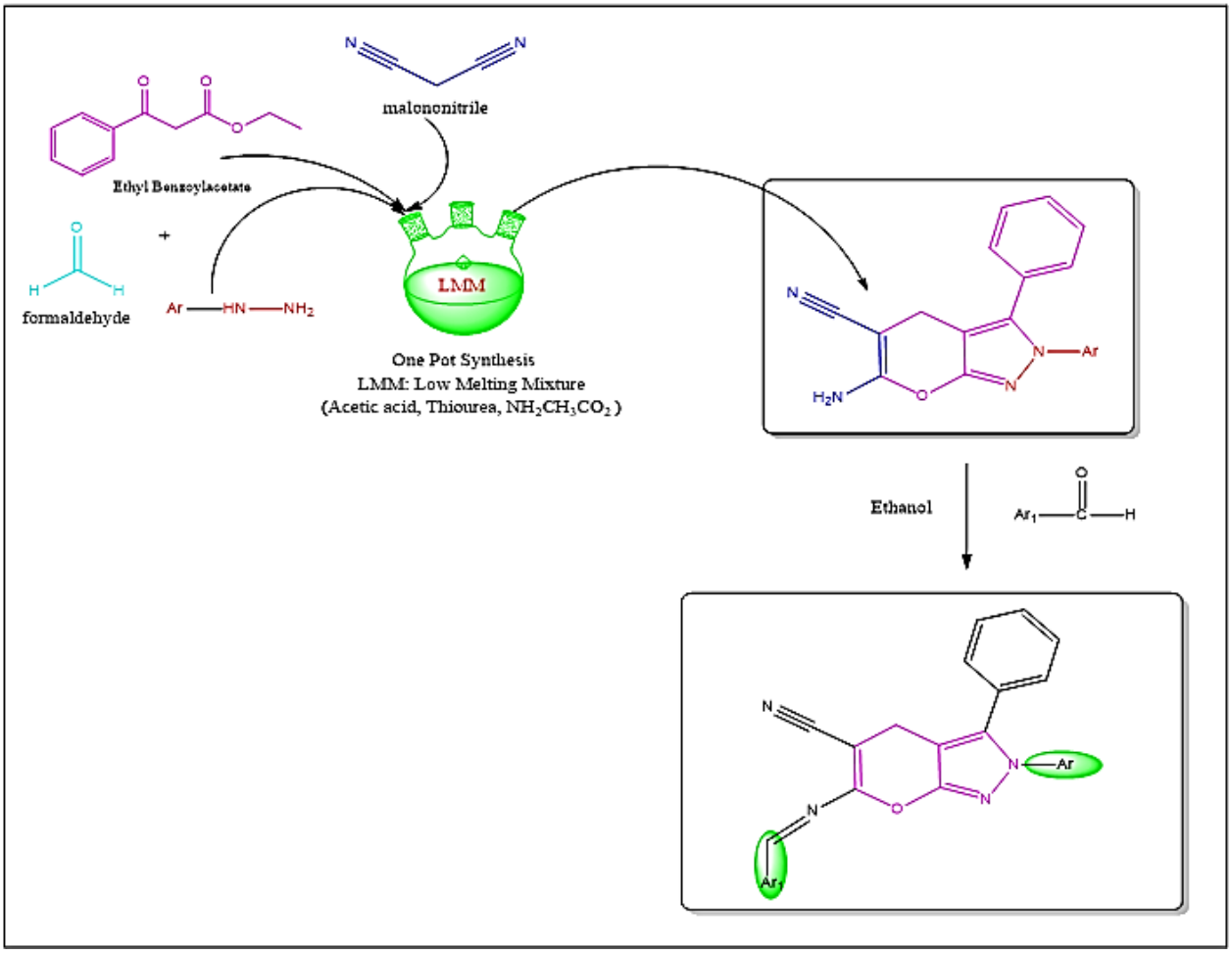

Figure 2: Proposed scheme for synthesis of Pyranopyrazole derivatives.

Results of Molecular Docking

Table 5: Results of Molecular Docking of pyranopyrazole derivatives with selected protein Glucosamine-6-phosphate synthase (PDB ID: 2VF5).

Compound	Active Amino Residues	Bond Lengths	Bond Category	Docking Score
SW1	SER303, ASN305, THR302, LEU484, VAL605, CYS300, ALA483, LEU480.	2.83, 3.18, 2.91, 3.84, 3.74, 3.74, 5.60, 4.92, 4.26, 4.58, 3.72, 5.45	Conventional Hydrogen Bond, Halogen, Pi-Donor Hydrogen Bond, Pi-Sigma, Pi-Sulfur, Amide-Pi Stacked, Alkyl, Pi-Alkyl.	-8.5
SW2	SER303, GLY301, LEU484, TYR304, LYS487.	2.36, 3.67, 3.84, 3.68, 4.99, 5.38 5.045, 4.56	Hydrogen Bond, Hydrophobic.	-8.5
SW3	GLN348, SER349, ALA602, GLY301, ASP354, VAL605, ILE326, CYS300.	2.49, 2.40, 1.87, 1.82, 3.28, 3.93, 3.99, 3.63, 4.28, 4.73, 4.33, 5.12, 4.86, 5.00	Conventional Hydrogen Bond, Carbon Hydrogen Bond, Pi-Anion, Pi-Sigma, Alkyl, Pi-Alkyl.	-9.1
SW4	SER303, GLY301, THR302, THR352, LEU480, LEU484, LYS487.	2.46, 3.49, 3.14, 3.67, 3.69, 3.91, 4.29, 4.91, 4.86, 4.65.	Conventional Hydrogen Bond, Carbon Hydrogen Bond, Pi-Sigma, Alkyl, Pi-Alkyl.	-9.0
SW5	THR302, SER303, LYS487, ALA602, LEU484, CYS300, ILE326.	2.80, 1.91, 2.33, 3.30, 3.57, 4.76, 4.14, 5.25.	Conventional Hydrogen Bond, Carbon Hydrogen Bond, Pi-Sigma, Alkyl, Pi-Alkyl.	-8.9
SW6	THR302, ASN305, SER401, GLY301, SER303, LEU484, LYS487, LEU601.	2.17, 2.33, 2.10, 2.75, 3.76, 3.48, 3.47, 5.72, 5.18, 5.49, 4.44, 5.24, 4.13	Conventional Hydrogen Bond, Carbon Hydrogen Bond, Pi-Pi T-shaped, Pi-Alkyl.	-9.4
SW7	SER303, LYS487, THR302, ALA602, LEU484, CYS300.	2.59, 2.57, 3.36, 3.50, 3.73, 4.74.	Conventional Hydrogen Bond, Carbon Hydrogen Bond, Pi-Sigma, Alkyl.	-8.8
SW8	THR352, LYS603, LEU484, LYS487, ILE326.	2.57, 3.29, 3.69, 3.98, 5.43, 4.583, 5.42	Conventional Hydrogen Bond, Carbon Hydrogen Bond, Pi-Sigma, Alkyl, Pi-Alkyl.	-8.9
SW9	LYS603, LEU484, ILE326.	3.47, 3.49, 4.30, 5.41	Carbon Hydrogen Bond, Pi-Sigma, Alkyl, Pi-Alkyl.	-8.7
SW10	ARG472, ASP548, ALA572, ALA551.	4.49, 3.87, 3.64, 4.29, 4.09, 4.44, 5.43.	Pi-Cation, Pi-Anion, Alkyl, Pi-Alkyl.	-8.4
Native Ligand	SER34, SER349, GLU488, LEU601, CYS300.	2.09, 1.699, 3.69, 4.98, 5.44	Conventional Hydrogen Bond, Carbon Hydrogen Bond, Alkyl, Pi-Alkyl.	-7.8

In silico ADME properties of designed pyranopyrazole derivatives SW1-SW10 were evaluated to predict pharmacokinetic profiles and drug-likeness as presented in Table 3. GI absorption was variable as some compounds SW1, SW2 and SW10 displayed high GI abs and thus have good potential for oral bioavailability while others such as SW3, SW4, SW5, SW6, SW7, SW8 and SW9 showed poor GI absorption. None of these compounds demonstrated the ability to cross BBB, which reduces the risk of central nervous system side effects and is a desirable property for antibacterial drugs. SW8 only demonstrated substrate activity for P-gp. SW7 and SW10 showed no inhibition of CYP2D6, but all three were somewhat pregnenolone-16-alpha-carbonitrile inducers. All compounds were mostly inhibitors of CYP2C19 and CYP2C9, with variable effects on other CYP enzymes. For example, SW4 and SW6 also showed inhibition of CYP3A4, thus indicating drug-drug interactions when the drugs were used in combination with other drugs metabolized by the enzyme. The skin permeability (Log Kp) values generally indicated poor skin permeability for all compounds whereas SW8 resulted in the highest value at (-3.84 cm/s) whereas the least value of (-6.23 cm/s) was contributed by SW4 and SW6 which meant minimal potential for transdermal delivery.

The drug-likeness assessment by Ghose, Egan and Muegge, as well as the bioavailability scores, not only justify but also emphasize the potential of these derivatives as candidate drugs. A majority of the compounds cleared these drug-likeness criteria, while SW1, SW2, SW7 and SW10 passed all the criteria and scored a bioavailability of 0.55, which indicates moderate oral bioavailability. SW3, SW4, SW5, SW6, SW8 and SW9 have poor bioavailability scores of 0.17; this could indicate a problem

Results of *In vitro* Antibacterial Activity

Table 6: Results of *In vitro* Antibacterial activity.

Compound	Code No.	Concentration (µg/mL)	Zone of Inhibition (mm)	
			Escherichia coli	*Staphylococcus aureus*
SW1	F1	25	8.4±0.3	9.6±0.3
	F2	50	12.8±0.8	13.2±0.2
	F3	100	18.2±0.3	20.3±0.7
SW2	F1	25	7.3±0.2	9.4±0.8
	F2	50	11.3±0.9	13.4±0.7
	F3	100	18.3±0.6	19.6±0.9
SW3	F1	25	8.2±0.3	9.3±0.3
	F2	50	12.9±0.2	11.4±0.5
	F3	100	19.3±-.4	20.3±0.2
SW4	F1	25	10.8±0.2	11.9±0.3
	F2	50	13.6±0.4	13.4±0.5
	F3	100	20.8±0.3	20.2±0.7
SW5	F1	25	9.4±0.1	8.7±0.3
	F2	50	13.2±0.4	11.7±0.7
	F3	100	19.3±0.8	18.6±0.8
SW6	F1	25	9.5±0.2	10.2±0.3
	F2	50	14.6±0.5	15.2±0.6
	F3	100	20.3±0.7	21.3±0.8
SW7	F1	25	7.3±0.9	8.4±0.5
	F2	50	13.1±0.7	11.3±0.8
	F3	100	17.8±0.3	16.3±0.4
SW8	F1	25	8.4±0.2	9.3±0.5
	F2	50	12.2±0.4	13.9±0.8
	F3	100	18.4±0.8	19.3±0.2
SW9	F1	25	6.4±0.3	7.6±0.9
	F2	50	10.3±0.2	14.2±0.5
	F3	100	14.4±0.8	18.3±0.3
SW10	F1	25	7.2±0.7	7.2±0.4
	F2	50	12.5±0.5	14.4±0.7
	F3	100	16.8±0.2	18.2±0.4
MS (Ciprofloxacin)	F1	25	12.8±0.3	12.3±0.1
	F2	50	17.4±0.6	18.2±0.2
	F3	100	24.8±0.8	23.7±0.4

Values are expressed in mean±SD, (n=3).

with attaining sufficient systemic levels. This improved insight from *in silico* ADME prediction of the pharmacokinetics and drug-likeness of pyranopyrazole derivatives helps point the way for further optimization and development.

The *in silico* toxicity analysis of designed pyranopyrazole derivatives (SW1-SW10) provided useful information concerning their potential toxicological profiles, which are represented in Table 4. All compounds showed LD_{50} values between 900 and 1190 mg/kg, confirming them under toxicity class 4, that is, relatively low acute toxicity. Accordingly, the compounds

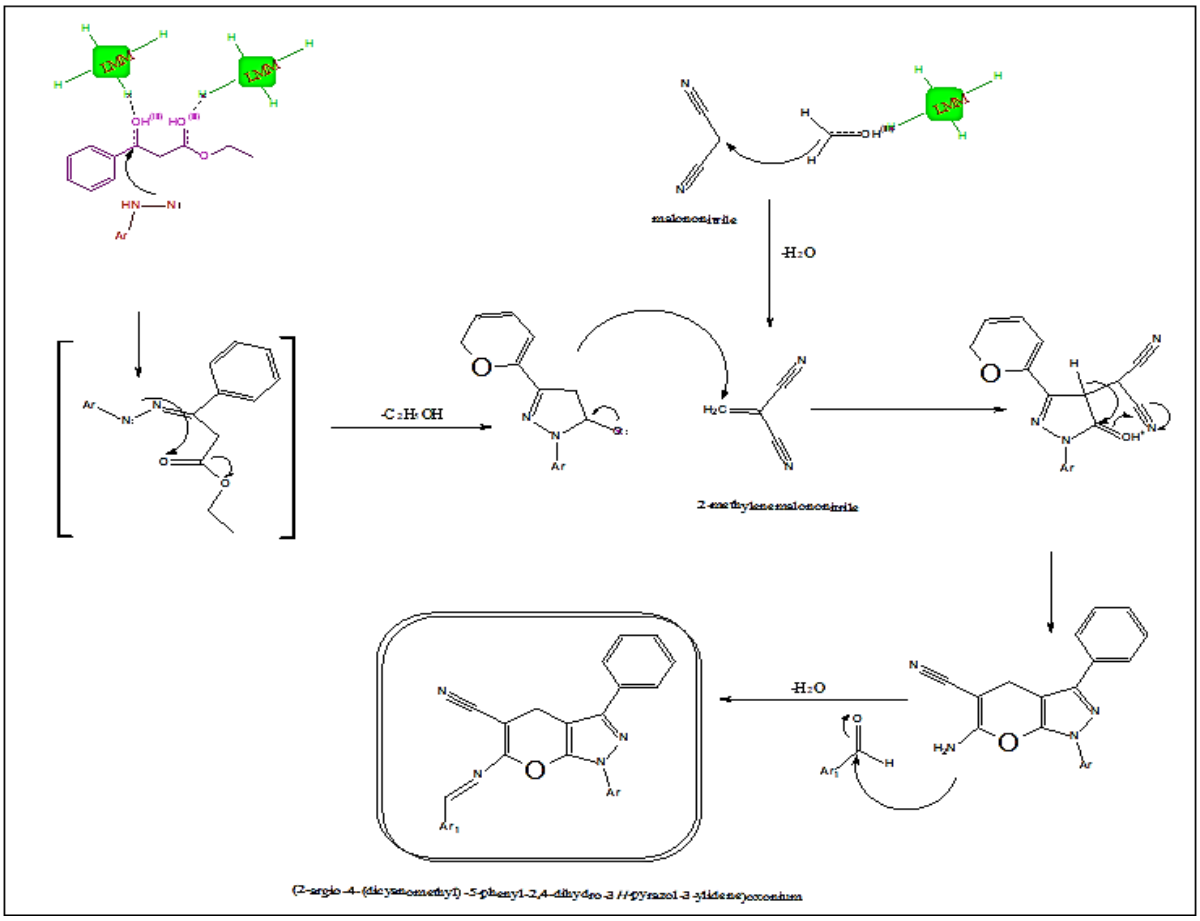

Figure 3: Mechanism of proposed scheme for synthesis ofPyranopyrazole derivatives.

are relatively safe at higher doses. Accuracy in prediction of some compounds was lower, for instance SW4 and SW6 with 23.78% and 23.32% respectively. Their correctness needs more validation from experiments. Specific toxicities have been demonstrated with some compounds such as active predictions for hepatotoxicity, carcinogenicity, immunotoxicity, mutagenicity and cytotoxicity. For instance, active predictions have been found among compounds SW1, SW2, SW3, SW4, SW5, SW6 and SW7 concerning hepatotoxicity with a probability level of approximately 0.55-0.69, meaning the probability of causing liver damage. Carcinogenicity was mostly non-active for most of the compounds except SW3 and SW4 that were active with probabilities ranging between 0.53-0.55. Immunotoxicity was observed to vary differently depending on the compound types, including SW3 and SW4 having higher probabilities (0.83-0.94), which might suggest immunosuppression. Mutagenicity was highly evident with most being predicted as active for SW3, SW5, SW6 and SW7 at a probability range of 0.71-0.97 that may pose possible risks in genetic mutation. Many compounds, including SW5, were also prone to cytotoxicity. Such *in silico* predictions of toxicity indicated that it has 0.93% chances of being cytotoxic. Such *in silico* toxicity predictions will define safety profiles for the pyranopyrazole derivatives. The fact that pyranopyrazoles in this study exhibited low acute toxicity values in an LD_{50} is encouraging. However, active predictions of specific toxicities strictly indicate that experimental validation is necessary. These insights could likely guide the structural optimization of these derivatives, so made with the design to remove potential toxic effects and improve safety and efficacy in antibacterial applications.

The molecular docking results of the pyranopyrazole derivatives with the target protein glucosamine-6-Phosphate synthase (PDB ID: 2VF5) were important for understanding how such compounds might interact with the protein and, therefore, be effective as antibacterial agents (Table 5). Of these, SW6 had the highest docking score of -9.4 and indicated the greatest affinity to the active site of GlmS. Indeed, the affinity can be rationalized by numerous conventional hydrogen bonds, carbon-hydrogen bonds and Pi-Pi T-shaped interactions that engage crucial active amino residues, including THR302, ASN305, SER401 and LEU484. Other Pi-Alkyl interactions contribute majorly to the stabilization of the complex. This means that SW6 can effectively interact stably at the binding site and inhibit the enzyme, as provided in Figure 5. SW3 and SW4 also exhibited high binding capacities with the docking scores of -9.1 and -9.0, respectively. Docking analysis reveals that SW3 interacts with critical residues such as GLN348, SER349 and ALA602 through the conventional hydrogen bonds and Pi-Anion interactions, as given in Figure 6. SW4 forms several hydrogen bonds with residues such as SER303

and GLY301, hence making it have high binding affinity (Figure 7). These make the enzyme-inhibitor complex more stable and may contribute to good inhibition of GlmS. Other compounds such as SW5, SW7 and SW8 also had docking scores in between -8.8 to -8.9, though lower than that of SW4, suggesting moderate binding affinities. Interestingly, the natural ligand, Ciprofloxacin, had a docking score of -7.8 which was lower than all the pyranopyrazole derivatives, indicating that these designed compounds may have higher inhibitory activity than the known antibacterial agent. Mahmoud M. Abdelatty *et al.*, 2023 found that their pyranopyrazole derivatives 3d and 4b were strongly active against *Bacillus subtilis* and *Staphylococcus aureus* with good interactions with tyrosyl-tRNA synthetase. Another set of compounds we isolated and characterized were called SW6 and SW4, which we identified to be prospective potent inhibitors of glucosamine-6-phosphate synthase displaying significant antibacterial activity against *Escherichia coli* and *Staphylococcus aureus*.

Binding interaction analyses further support the conclusions. For example, SW1 and SW2, with docking scores of -8.5, bind to the active site residues SER303, ASN305 and LEU484 using traditional hydrogen bonds and hydrophobic interactions to stabilize the binding process. SW10, which has the lowest docking score of -8.4 of its analogs, still interacts with potential structures such as Pi-Cation and Pi-Anion through ARG472 and ASP548. In Figures 5-8, the analysis indicates that comparative modes of binding as revealed through the pyranopyrazole derivatives form not only more diverse but stronger interactions with the residues of the active site of GlmS than the native ligand itself. It thus suggests that these derivatives have a greater potential to act as potent inhibitors of GlmS and therefore for effective antibacterial activity.

A highly efficient one-pot, multicomponent reaction strategy has been employed for the synthesis of the pyranopyrazole derivatives SW1-SW10. This method benefits from an approach in which ethyl benzoylacetate, substituted phenyl hydrazine, formaldehyde and malononitrile react together in the presence of a catalyst system made up of acetic acid, thiourea and ammonium acetate. The reaction conditions were such that stirring at room temperature followed by refluxing with the substituted

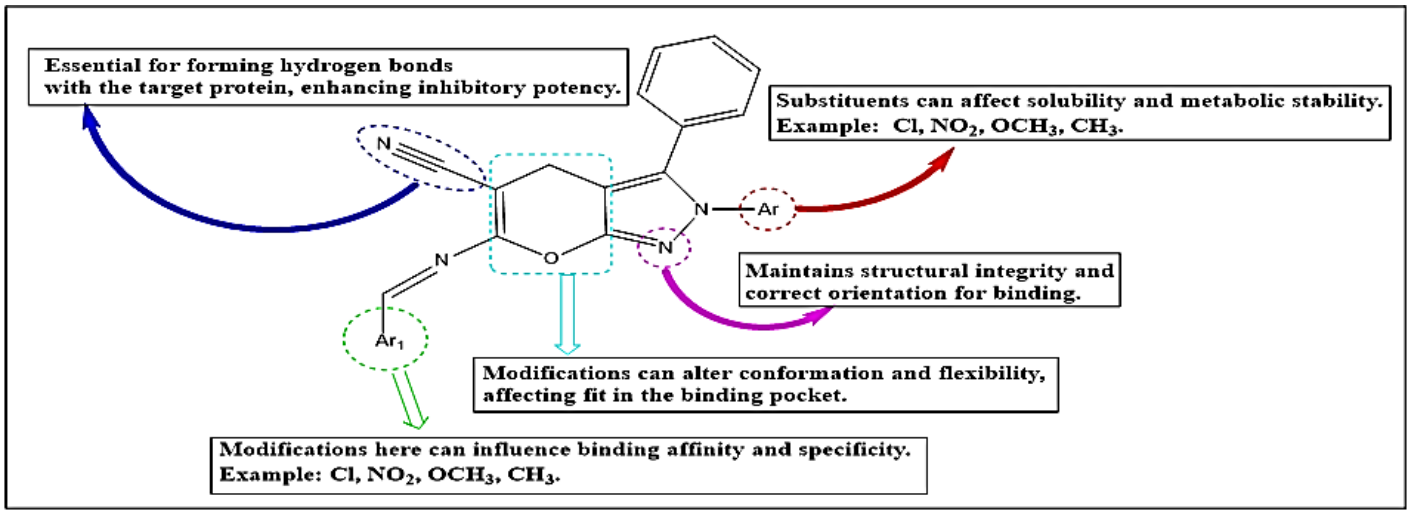

Figure 4: Chemistry of pyranopyrazole derivatives.

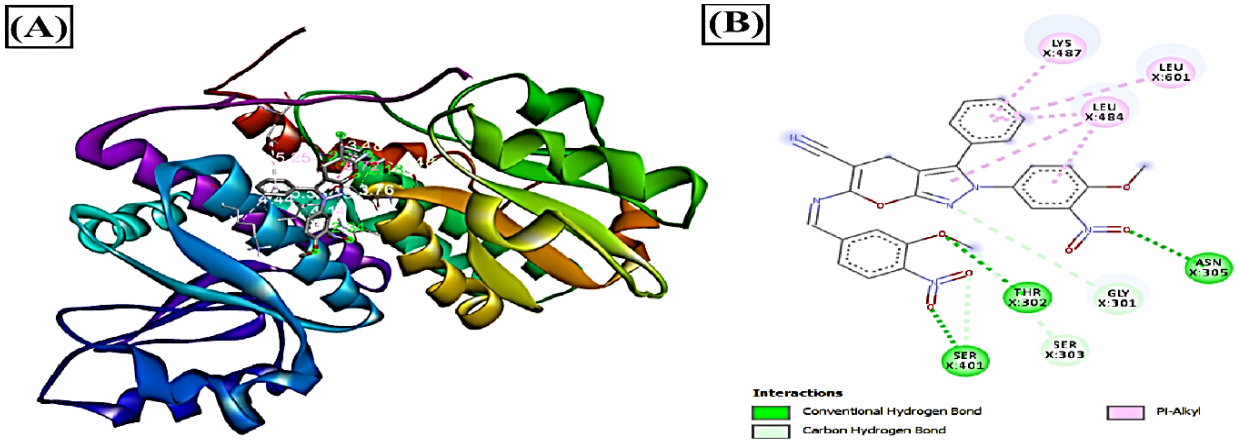

Figure 5: Binding of SW6 compound to active site of Glucosamine-6-phosphate (PDB ID- 2VF5) (A) along with the 2D binding diagram (B).

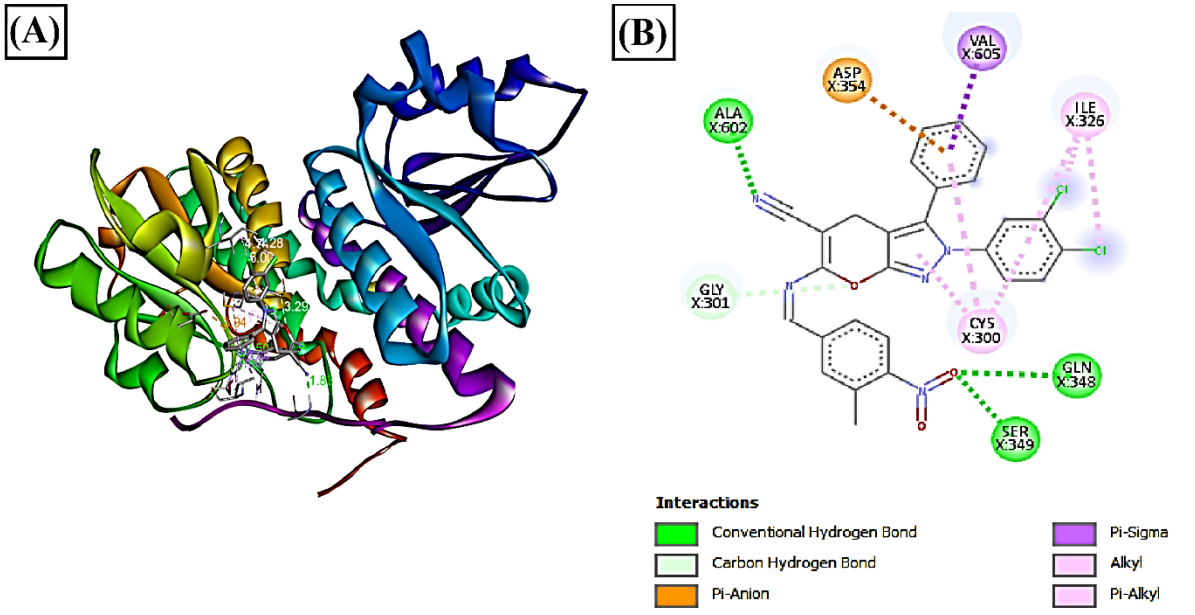

Figure 6: Binding of SW3 compound to active site of Glucosamine-6-phosphate (PDB ID-2VF5) (A) along with the 2D binding diagram (B).

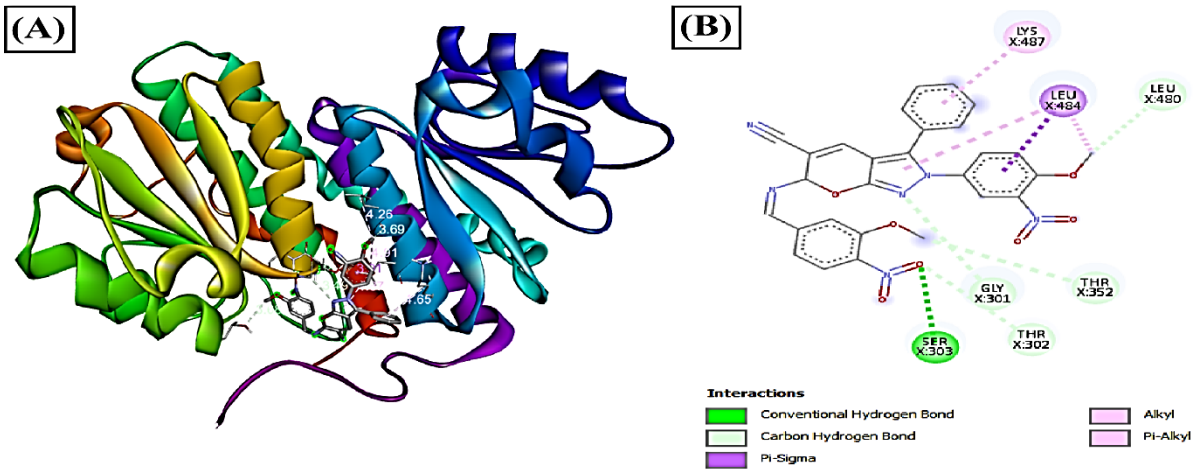

Figure 7: Binding of SW4 compound to active site of Glucosamine-6-phosphate (PDB ID- 2VF5) (A) along with the 2D binding diagram (B).

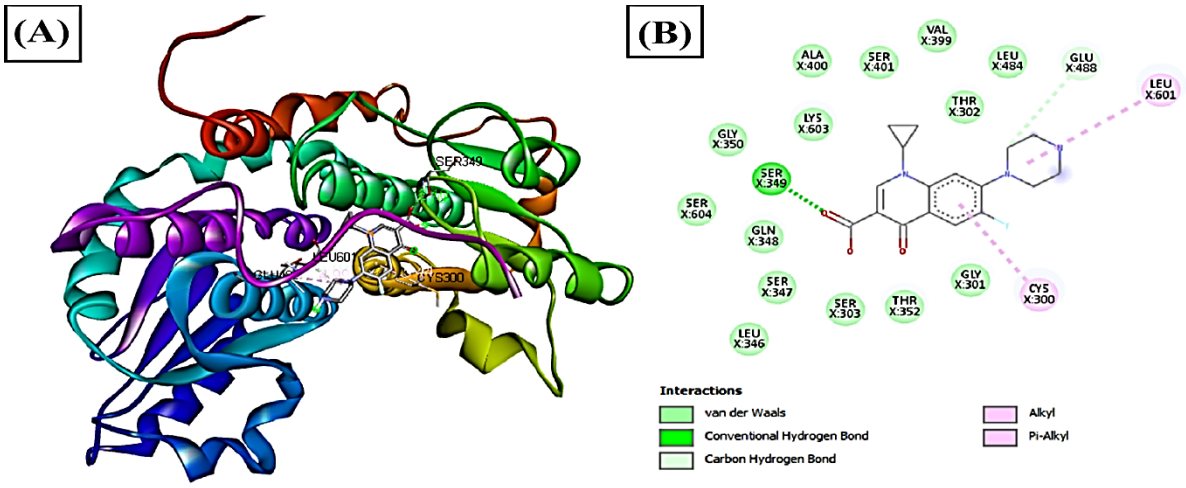

Figure 8: Binding of Native Ligand to active site of Glucosamine-6-phosphate (PDB ID- 2VF5) (A) along with the 2D binding diagram (B).

benzaldehyde made it easier to form the desired structure of pyranopyrazoles with minimal complexity in the procedure and high yield. The structural integrity as well as purity of the compound was verified by 1H NMR, FTIR and MS techniques to ascertain the accuracy in the product formation. Letcy V. Theresa *et al*. reported a green route for the synthesis of the pyranopyrazole derivatives by employing a low melting mixture of lactic acid, urea and NH_4Cl (Theresa *et al*., 2021). The author mentioned that this is a simple, solvent-free, one-pot reactions producing high purity with ease workup and shorter reaction times. Yield was very high and this process at room temperature showed considerable improvement over the traditional synthesis routes. This approach not only simplified the synthesis process but also demonstrated its potential in yielding compounds with significant potential for biological activity. The efficiency of this method, coupled with the very high purity of the resultant product, makes it a useful strategy in generating diverse pyranopyrazole derivatives as part of current sustainable and practical synthetic methodologies.

The synthesized pyranopyrazole derivatives, SW1-SW10, were evaluated for their *in vitro* antibacterial activity against the bacteria *Escherichia coli* and *Staphylococcus aureus* through zones of inhibition at various concentrations: 25 µg/mL, 50 µg/mL and 100 µg/mL. Results given in Table 6 indicated that in all the compounds examined, a direct boost in antibacterial activity was observed with concentration, but remarkable differences were seen in the efficacy between the compounds and the two pathogens used in this study. Among the derivatives, SW6 exhibited the highest antibacterial potency with zone sizes of inhibition measured at 9.5±0.2 mM, 14.6±0.5 mM and 20.3±0.7 mM against *E. coli* and 10.2±0.3 mM, 15.2±0.6 mM and 21.3±0.8 mM against *S. aureus* at concentrations of 25 µg/mL, 50 µg/mL and 100 µg/mL, respectively. This potential activity seems to correlate with the strong docking score of -9.4 against glucosamine-6-phosphate synthase and, hence, tight binding and effective inhibition of this target enzyme that is necessary for the synthesis of bacterial cell walls. In contrast to SW4, zones of inhibition reached high antibacterial efficacy at 20.8±0.3 mM *E. coli* and at 20.2±0.7 mM *S. aureus* at a concentration of 100 µg/mL, well within accord with a favorable docking score of -9.0.

The series of derivatives containing SW3 and SW5 also displayed significant antibacterial activity with zones of inhibition almost comparable to those observed by the analogues SW6 and SW4, which originates from their relatively high scores of docking and proper interaction with the target enzyme. Compounds like SW9 and SW10, with their docking scores as low as -8.7 and -8.4, showed significantly reduced antibacterial activity, with zones of inhibition much smaller compared to the best derivatives. This trend can point out the connection of docking scores with antibacterial efficiency; in other words, the better the interaction of this compound with glucosamine-6-phosphate synthase, the more this compound can be effective as an inhibitor against bacterial growth. The activity of ciprofloxacin, an established antibiotic drug, was also tested for comparison. With zones of inhibition values of 12.8±0.3 mM, 17.4±0.6 mM and 24.8±0.8 mM against *E. coli*, 12.3±0.1 mM, 18.2±0.2 mM and 23.7±0.4 mM versus *S. aureus* at 25 µg/mL, 50 µg/mL and 100 µg/mL, respectively. None of synthetic derivatives were more effective than ciprofloxacin, however, compounds SW6 and SW4 demonstrated a good outlook for further optimization and investigation. The pyranopyrazole derivatives, in particular the compounds SW6 and SW4, seemed promising and resembled potential effective antibacterial agents.

CONCLUSION

The synthesized pyranopyrazole derivatives demonstrated good potential for activity as an antibacterial against both *Escherichia coli* and *Staphylococcus aureus*. Among them, SW6 was the one most promising when *in silico* molecular docking was considered and it also demonstrated the highest *in vitro* antibacterial activity. These compounds showed strong binding affinities to glucosamine-6-phosphate synthase correlating well with effective inhibition of bacterial growth. These complexes even more establish their drug-like potential against potential toxicities with bioavailability through *in silico* ADME and toxicity analyses; however, some still require optimization of those particular aspects. In conclusion, the research indicates that pyranopyrazole derivatives, especially SW6 and SW4, are promising lead compounds in the development of novel antibacterial therapies, owing to the urgent need for the development of new drugs to address antibiotic-resistant bacterial strains.

ACKNOWLEDGEMENT

The authors express gratitude to principal and staff of Sanjivani College of Pharmaceutical Education and Research, Kopargaon, India, for providing the necessary facilities for the completion of this research work.

CONFLICT OF INTEREST

The author declares that there is no conflict of interest.

ABBREVIATIONS

GlmS: Glucosamine 6 phosphate synthase; **GI:** Gastrointestinal; **BBB:** Blood Brain Barrier; **Pgp:** P glycoprotein; **CYP:** Cytochrome P450; **LD_{50}:** Lethal Dose 50%; **HBD:** Hydrogen Bond Donor; **HBA:** Hydrogen Bond Acceptor; **Mol. Wt.:** Molecular Weight; **Log P:** Partition Coefficient; **TPSA:** Total Polar Surface Area; **ADMET:** Absorption, Distribution, Metabolism, Excretion and Toxicity; **Log Kp:** Logarithm of Skin Permeation Coefficient; FTIR: Fourier transform infrared spectroscopy; **NMR:** Nuclear magnetic resonance spectroscopy; **MS:** Mass spectrometry; **TMS:**

Tetramethylsilane; **TLC:** Thin layer chromatography; **DMSO:** Dimethyl sulfoxide.

REFERENCES

Abdelatty, M. M., Farag, Z. R., El Hassane, A., Moustapha, M. E., & Makhlouf, A. A. (2023a). Yossef AM. Synthesis, antimicrobial studies and molecular docking simulation of novel pyran, pyrazole and pyranopyrazole derivatives. Journal of Chemistry, 2023(1), Article 6623445. https://doi.org/10.1155/2023/6623445

Abdelatty, M. M., Farag, Z. R., El Hassane, A., Moustapha, M. E., & Makhlouf, A. A. (2023b). Yossef AM. Synthesis, antimicrobial studies and molecular docking simulation of novel pyran, pyrazole and pyranopyrazole derivatives. Journal of Chemistry;2023(1), Article 6623445. https://doi.org/10.1007/s11030-017-9738-7

Abdelazeem, N. M., Aboulthana, W. M., Elshahid, Z. A., El-Hussieny, M., & Al-Ashmawy, A. A. K. (2024, August 15). Synthesis and biological (*in vitro* and *in silico*) screening of the 4-aryl-fused pyranopyrazole derivatives as enzyme (α-amylase, α-glucosidase, acetylcholinesterase & proteinase) inhibitors with anti-oxidant and cytotoxic activities. Journal of Molecular Structure, 1310, Article 138224. https://doi.org/10.1016/j.molstruc.2024.138224

Agrwal, A., Pathak, R. K., & Kasana, V. (2022, January 1). Molecular docking and antibacterial studies of pyranopyrazole derivatives synthesized using [Pap-Glu@ Chi] biocatalyst through a greener approach. Arabian Journal for Science and Engineering, 47(1), 347–363. https://doi.org/10.1007/s13369-021-05377-1

Allayeh, A. K., El-Boghdady, A. H., Said, M. A., Saleh, M. G. A., Abdel-Aal, M. T., & Abouelenein, M. G. (2024, February 2). Discovery of pyrano [2, 3-c] pyrazole Derivatives as Novel Potential Human Coronavirus Inhibitors: Design, Synthesis, *in silico, in vitro* and ADME Studies. Pharmaceuticals, 17(2), 198. https://doi.org/10.3390/ph17020198

Banerjee, P., Eckert, A. O., Schrey, A. K., & Preissner, R. (2018, July 2). ProTox-II: A webserver for the prediction of toxicity of chemicals. Nucleic Acids Research, 46(W1), W257–W263. https://doi.org/10.1093/nar/gky318

Banerjee, P., & Ulker, O. C. (2022, September 2). Combinative *ex vivo* studies and *in silico* models ProTox-II for investigating the toxicity of chemicals used mainly in cosmetic products. Toxicology Mechanisms and Methods, 32(7), 542–548. https://doi.org/10.1080/15376516.2022.2053623

Batool, A., Parveen, S., Shafiq, N., Rashid, M., Salamatullah, A. M., Ibenmoussa, S., & Bourhia, M. (2024, February 15). Computational study of ADME-Tox prediction of selected phytochemicals from *Punica granatum* peels. Open Chemistry, 22(1), Article 20230188. https://doi.org/10.1515/chem-2023-0188

Beneito-Cambra, M., Gareil, P., Badet, B., Badet-Denisot, M.-A., & Delaunay, N. (2018, January 1). First investigations for the characterization of glucosamine-6-phosphate synthase by capillary electrophoresis. Journal of Chromatography. B, Analytical Technologies in the Biomedical and Life Sciences, 1072, 130–135. https://doi.org/10.1016/j.jchromb.2017.11.015

Bennett, A. M., Shippy, D. C., Eakley, N., Okwumabua, O., & Fadl, A. A. (2016, August). Functional characterization of glucosamine-6-phosphate synthase (GlmS) in *Salmonella enterica* serovar Enteritidis. Archives of Microbiology, 198(6), 541–549. https://doi.org/10.1007/s00203-016-1212-x

Besser, J., Carleton, H. A., Gerner-Smidt, P., Lindsey, R. L., & Trees, E. (2018, April 1). Next-generation sequencing technologies and their application to the study and control of bacterial infections. Clinical Microbiology and Infection, 24(4), 335–341. https://doi.org/10.1016/j.cmi.2017.10.013

Butt, S. S., Badshah, Y., Shabbir, M., & Rafiq, M. (2020, June 19). Molecular docking using chimera and autodock vina software for nonbioinformaticians. JMIR Bioinformatics and Biotechnology, 1(1), Article e14232. https://doi.org/10.2196/14232

Damayanti, F. D., & Setiawan, R. A., Maretha TL, andhani TV, Awwaluddin F, Prihantono RP, Jamil AS. *In silico* Analysis Potential of *Curcuma zedoaria* As a Candidate for Degenerative Disease Therapy. EKSAKTA: Journal of Sciences and Data Analysis. 2022 Aug 31. https://doi.org/10.20885/EKSAKTA.vol3.iss2.art3.

Eberhardt, J., Santos-Martins, D., Tillack, A. F., Forli, S., & AutoDock, V. 1.2. 0. (2021, July 19). New docking methods, expanded force field and python bindings. Journal of Chemical Information and Modeling, 61(8), 3891–3898. https://doi.org/10.1021/acs.jcim.1c00203

El-Hachem, N., Haibe-Kains, B., Khalil, A., Kobeissy, F. H., & Nemer, G. (2017). AutoDock and AutoDockTools for protein-ligand docking: Beta-site amyloid precursor protein cleaving enzyme 1 (BACE1) as a case study. Neuroproteomics. Methods and Protocols, 391–403.

Farooq, S., & Ngaini, Z. (2024, February 26). Recent synthesis of mono-& bis-pyranopyrazole derivatives. ChemistrySelect, 9(8), Article e202400028. https://doi.org/10.1002/slct.202400028

Fikrika, H., Ambarsari, L., & Sumaryada, T. (2016) (Vol. 31, No. 1, p. 012009). Molecular docking studies of catechin and its derivatives as anti-bacterial inhibitor for glucosamine-6-phosphate synthase. InIOP Conference Series: Earth and Environmental Science, 31. https://doi.org/10.1088/1755-1315/31/1/012009

Fisher, R. A., Gollan, B., & Helaine, S. (2017, August). Persistent bacterial infections and persister cells. Nature Reviews. Microbiology, 15(8), 453–464. https://doi.org/10.1038/nrmicro.2017.42

Forli, S., Huey, R., Pique, M. E., Sanner, M. F., Goodsell, D. S., & Olson, A. J. (2016, May). Computational protein-ligand docking and virtual drug screening with the AutoDock suite. Nature Protocols, 11(5):905-19, 905–919. https://doi.org/10.1038/nprot.2016.051

Fouda, A. M., El-Nassag, M. A. A., Elhenawy, A. A., Shati, A. A., Alfaifi, M. Y., Elbehairi, S. E. I., Alam, M. M., & El-Agrody, A. M. (2022, February 5). Synthesis of 1, 4-dihydropyrano [2, 3-c] pyrazole derivatives and exploring molecular and cytotoxic properties based on DFT and molecular docking studies. Journal of Molecular Structure, 1249, Article 131555. https://doi.org/10.1016/j.molstruc.2021.131555

Foulquier, E., Pompeo, F., Byrne, D., Fierobe, H.-P., & Galinier, A. (2020, September 29). Uridine diphosphate N-acetylglucosamine orchestrates the interaction of GlmR with either YvcJ or GlmS in *Bacillus subtilis*. Scientific Reports, 10(1), Article 15938. https://doi.org/10.1038/s41598-020-72854-2

Gadkari, Y. U., Hatvate, N. T., & Telvekar, V. N. (2021, October). Concentrated solar radiation-assisted one-pot/multicomponent synthesis of pyranopyrazole derivatives under neat condition. Research on Chemical Intermediates, 47(10), 4245–4255. https://doi.org/10.1007/s11164-021-04530-7

Gaillard, T. (2018, July 10). Evaluation of AutoDock and AutoDock Vina on the CASF-2013 benchmark. Journal of Chemical Information and Modeling, 58(8), 1697–1706. https://doi.org/10.1021/acs.jcim.8b00312

Jernigan, J. A., Hatfield, K. M., Wolford, H., Nelson, R. E., Olubajo, B., Reddy, S. C., McCarthy, N., Paul, P., McDonald, L. C., Kallen, A., Fiore, A., Craig, M., & Baggs, J. (2020, April 2). Multidrug-resistant bacterial infections in US hospitalized patients, 2012–2017. The New England Journal of Medicine, 382(14), 1309–1319. https://doi.org/10.1056/NEJMoa1914433

Jia, Q., Song, Q., Li, P., & Huang, W. (2019, July). Rejuvenated photodynamic therapy for bacterial infections. Advanced Healthcare Materials, 8(14), Article e1900608. https://doi.org/10.1002/adhm.201900608

Khan, M. A., Göpel, Y., Milewski, S., & Görke, B. (2016, June 15). Two small RNAs conserved in Enterobacteriaceae provide intrinsic resistance to antibiotics targeting the cell wall biosynthesis enzyme glucosamine-6-phosphate synthase. Frontiers in Microbiology, 7, 908. https://doi.org/10.3389/fmicb.2016.00908

Kurma, S., Nukala, S. K., Thirukovela, N. S., Badithapuram, V., Dasari, G., & Bandari, S. (2024, September 13). Design and synthesis of some new quinoxaline-1, 2, 4-oxadiazole-amide conjugates as EGFR targeting agents and ADMET studies. Polycyclic Aromatic Compounds, 44(8), 5504–5517. https://doi.org/10.1080/10406638.2023.2265027

Li, P., Li, K., Li, X., Zhao, F., Wang, R., & Wang, J. (2020, November). Improving enzyme activity of glucosamine-6-phosphate synthase by semi-rational design strategy and computer analysis. Biotechnology Letters, 42(11), 2319–2332. https://doi.org/10.1007/s10529-020-02949-3

Liu, X., & Ma, S. (2020, February 7). Recent development of glucosamine-6-phosphate derivatives as potential antibacterial agents. ChemistrySelect, 5(5), 1718–1727. https://doi.org/10.1002/slct.201904075

Makabenta, J. M. V., Nabawy, A., Li, C.-H., Schmidt-Malan, S., Patel, R., & Rotello, V. M. (2021, January). Nanomaterial-based therapeutics for antibiotic-resistant bacterial infections. Nature Reviews. Microbiology, 19(1), 23–36. https://doi.org/10.1038/s41579-020-0420-1

Mamaghani, M., & Hossein Nia, R. (2021, February 7). A review on the recent multicomponent synthesis of pyranopyrazoles. Polycyclic Aromatic Compounds, 41(2), 223–291. https://doi.org/10.1080/10406638.2019.1584576

Moosavi-Zare, A. R., Zolfigol, M. A., Salehi-Moratab, R., & Noroozizadeh, E. (2016, May 1). Catalytic application of 1-(carboxymethyl) pyridinium iodide on the synthesis of pyranopyrazole derivatives. Journal of Molecular Catalysis A: Chemical, 415, 144–150. https://doi.org/10.1016/j.molcata.2016.02.003

Morris, D. E., Cleary, D. W., & Clarke, S. C. (2017, June 23). Secondary bacterial infections associated with influenza pandemics. Frontiers in Microbiology, 8, 1041. https://doi.org/10.3389/fmicb.2017.01041

Niu, T., Liu, Y., Li, J., Koffas, M., Du, G., Alper, H. S., & Liu, L. (2018, August 23). Engineering a glucosamine-6-phosphate responsive glmS ribozyme switch enables dynamic control of metabolic flux in *Bacillus subtilis* for overproduction of N-acetylglucosamine. ACS Synthetic Biology, 7(10), 2423–2435. https://doi.org/10.1021/acssynbio.8b00196

Oner, E., Al-Khafaji, K., Mezher, M. H., Demirhan, I., Suhail Wadi, J., Belge Kurutas, E., Yalin, S., & Choowongkomon, K. (2023, November 24). Investigation of berberine and its derivatives in Sars Cov-2 main protease structure by molecular docking, PROTOX-II and ADMET methods: In machine learning and *in silico* study. Journal of Biomolecular Structure and Dynamics, 41(19), 9366–9381. https://doi.org/10.1080/07391102.2022.2142848

Piano, S., Singh, V., Caraceni, P., Maiwall, R., Alessandria, C., Fernandez, J., Soares, E. C., Kim, D. J., Kim, S. E., Marino, M., Vorobioff, J., Barea, R. C. R., Merli, M., Elkrief, L., Vargas, V., Krag, A., Singh, S. P., Lesmana, L. A., Toledo, C., International Club of Ascites Global Study Group. (2019, April 1). Epidemiology and effects of bacterial infections in patients with cirrhosis worldwide. Gastroenterology, 156(5), 1368–1380.e10. https://doi.org/10.1053/j.gastro.2018.12.005

Principi, N., Silvestri, E., & Esposito, S. (2019, May 8). Advantages and limitations of bacteriophages for the treatment of bacterial infections. Frontiers in Pharmacology, 10, 513. https://doi.org/10.3389/fphar.2019.00513

Ravi, L., & Kannabiran, K. (2016, June 1). A handbook on protein-ligand docking tool: AutoDock 4. Innovare Journal of Medical Sciences, 28–33.

Sharma, A., Chowdhury, R., Dash, S., Pallavi, B., & Shukla, P. (2015). Fast microwave assisted synthesis of pyranopyrazole derivatives as new anticancer agents. Current Microwave Chemistry, 3(1), 78–84. https://doi.org/10.2174/2213335602666150116233238

Silkenath, B., Kläge, D., Altwein, H., Schmidhäuser, N., Mayer, G., Hartig, J. S., & Wittmann, V. (2023, October 4). Phosphonate and Thiasugar analogues of glucosamine-6-phosphate: Activation of the glmS riboswitch and antibiotic activity. ACS Chemical Biology, 18(10), 2324–2334. https://doi.org/10.1021/acschembio.3c00452

Soukup, J. (2021, September 14). The glmS ribozyme and its multifunctional coenzyme glucosamine-6-phosphate. Ribozymes, 1, 91–115.

Theresa, L. V., Pradeep, S. D., Sebastian, D., & Sreekumar, K. (2021, January 1). Sustainable multicomponent one pot synthesis of pyranopyrazole derivatives in the presence of lactic acid: Urea: NH4Cl. Current Research in Green and Sustainable Chemistry, 4, Article 100194. https://doi.org/10.1016/j.crgsc.2021.100194

Yadav, M., Gope, L., Kumari, N., & Yadav, P. (2016, April 1). Corrosion inhibition performance of pyranopyrazole derivatives for mild steel in HCl solution: Gravimetric, electrochemical and DFT studies. Journal of Molecular Liquids, 216, 78–86. https://doi.org/10.1016/j.molliq.2015.12.106

Cite this article: Jadhav PB, Wagh SV, Dabhade MP. Design, Synthesis, *in silico* Molecular Docking, ADMET Analysis and *in vitro* Antibacterial Activity of Pyranopyrazole Derivatives as Potent Glucosamine-6-Phosphate Synthase Inhibitor. Int. J. Pharm. Investigation. 2025;15(3):873-87.